RSC Advances

PAPER

View Article Online
View Journal | View Issue

Cite this: *RSC Adv.*, 2023, **13**, 20229

Upconversion nanoparticle-based aptasensor for rapid and ultrasensitive detection of *Staphylococcus aureus* by low-speed centrifugation†

Na Li,‡[a] Ying Zhang,‡[ab] Tiancheng Wei,[a] Tao Yang,[c] Qing Bao,[c] Qichao Cheng,[a] Chuanbin Mao,[c] Yajun Shuai[a] and Mingying Yang*[a]

Opportunistic foodborne pathogens such as *Staphylococcus aureus* (*S. aureus*) can cause a wide variety of threats to public health. There is an urgent clinical need for a fast, simple, low-cost, and sensitive method. Here, we designed a fluorescence-based aptamer biosensor (aptasensor) for *S. aureus* detection using core–shell structured upconversion nanoparticles (CS-UCNPs) as a beacon. A *S. aureus*-specific aptamer was modified on the surface of CS-UCNPs for binding pathogens. The *S. aureus* bound to CS-UCNPs can then be isolated from the detection system by simple low-speed centrifugation. Thus, an aptasensor was successfully established for the detection of *S. aureus*. The fluorescence intensity of CS-UCNPs correlated with the concentration of *S. aureus* within the range of 6.36×10^2 to 6.36×10^8 CFU mL^{-1}, resulting in the detected limit of *S. aureus* being 60 CFU mL^{-1}. The aptasensor performed well in real food samples (milk) with a detection limit of 146 CFU mL^{-1} for *S. aureus*. Furthermore, we applied our aptasensor in chicken muscles for *S. aureus* detection, and compared it with the plate count gold standard method. There was no significant difference between our aptasensor and the plate count method within the detected limit, while the time for the aptasensor (0.58 h) was shorter than that of the plate count method (3–4 d). Therefore, we succeeded in the design of a simple, sensitive and fast CS-UCNPs aptasensor for *S. aureus* detection. This aptasensor system would have the potential for the detection of a wide range of bacterial species by switching the corresponding aptamer.

Received 9th March 2023
Accepted 25th May 2023

DOI: 10.1039/d3ra01555f

rsc.li/rsc-advances

Introduction

Staphylococcus aureus (*S. aureus*), a harmful foodborne pathogen that is easily found in high-protein foods such as meat and milk, has been of wide concern in food safety.[1] The infections caused by *S. aureus* range from mild skin and soft tissue infections (such as boils and impetigo) to more serious illnesses (such as sepsis, pneumonia, and endocarditis).[2] Therefore, detecting the presence of *S. aureus* in food samples is the key element in reducing the risks associated with public health. Traditional *S. aureus* detection methods include culture-based methods[3] and PCR-based methods.[4] Culture-based methods remain the gold standard, but they require long incubation times, which can delay diagnosis and treatment. PCR-based methods are rapid and sensitive, but they are expensive and can produce false-positive or false-negative results. Hence, it is urgent to develop a sensitive, accurate and low-cost method for *S. aureus* detection.

To meet these needs, several biosensors based on aptamer,[5] phages,[6] and antibodies[7] have been designed for *S. aureus* detection. In particular, biosensors based on fluorescence, with their exceptional sensitivity, impressive efficiency, and swift analytic capabilities, have risen to prominence as a pervasive sensing modality in the examination and identification of low-concentration analytes. For example, Yao *et al.* developed a one-step fluorometric strategy in which carbon dots was used as the energy donor and gold nanoparticles as energy acceptor, the existence of *S. aureus* will recover the Fluorescence of the system; the LOD of the system was 10 CFU mL^{-1}.[8] Although these methods can provide accurate results, the quantum dots and fluorescence dyes used as signals have limitations in the actual sample detection, such as short fluorescence life, strong toxicity, background spontaneous fluorescence and so on.[9] Lanthanide-doped upconversion nanoparticles (UCNPs), with special optical properties including large anti-Stokes shift, clear

[a]*Zhejiang Provincial Key Laboratory of Utilization and Innovation of Silkworm and Bee Resources, Institute of Applied Bioresource Research, College of Animal Science, Zhejiang University, Hangzhou, China. E-mail: yangm@zju.edu.cn*

[b]*School of Life Sciences, Westlake University, Hangzhou 310024, Zhejiang, China*

[c]*School of Materials Science and Engineering, Zhejiang University, Hangzhou, 310058, P. R. China*

† Electronic supplementary information (ESI) available. See DOI: https://doi.org/10.1039/d3ra01555f

‡ Na Li and Ying Zhang made equal contribution in this study.

emission wavelengths and better photostability, have been considered as potential substitutes for quantum dots and organic fluorophores.[10] In recent years, aptamers have been well applied in biosensors based on UCNPs due to their superior performance.[11,12] Aptamers can be ssRNA or ssDNA targeting pathogenic bacteria and curl up when the 3D structure of the aptamer specifically binds to a small molecule on the surface of the pathogen.[13] Furthermore, recognition elements based on ssRNA or ssDNA have advantages, such as low cost, high stability at a large range of pH and temperature, nontoxicity, *etc.*[14]

At present, most of the sensing methods of *S. aureus* in the detection system combined with UCNPs and aptamers are realized through Förster resonance energy transfer (FRET). The FRET process requires both energy donor and energy acceptor, and that the donor's emission spectrum and the acceptor's absorption spectrum overlap. The operation process of such an experiment is undoubtedly complicated, which is not conducive to market promotion. hence, we demonstrated a biosensor based on centrifugal separation for *S. aureus* detection by using core–shell UCNPs (CS-UCNPs) as signal agents and *S. aureus*-specific aptamer as recognition agents (Fig. 1). We first synthesized the core UCNPs. The lifetime and fluorescence signal of UCNPs are highly dependent on their upconversion efficiencies.[15] To address this, we constructed UCNPs with the core–shell structure by coating core UCNPs with $NaYF_4$ shells to have a high energy transfer efficiency.[16] The functionalization of the CS-UCNPs with the *S. aureus*-specific aptamer resulted in an aptasensor for *S. aureus* detection. Compared with other FRET-based biosensors, we do not use a fluorescence quenching agent to cause fluorescence signal difference. Due to the large difference in diameter between the nanoparticles and the *S. aureus* (almost 30 times), it could be easy to separate them by centrifugation alone. In the absence of *S. aureus*, the precipitate was barely visible by low-speed centrifugation (3000 g, 5 min) and the fluorescence of the solution barely decreases. When *S. aureus* was present, aptasensors could bind specifically to the *S. aureus*. After the low-speed centrifugation (3000 g, 5 min) and separation, the precipitate (*S. aureus* and the binding aptasenors) cause a significant reduction in the fluorescence of the solution. Therefore, we were able to separate *S. aureus* by tracking the fluorescence intensity of aptasensors. Furthermore, we confirmed that the aptasensor can be used to detect *S. aureus* from biological samples (commercial milk).

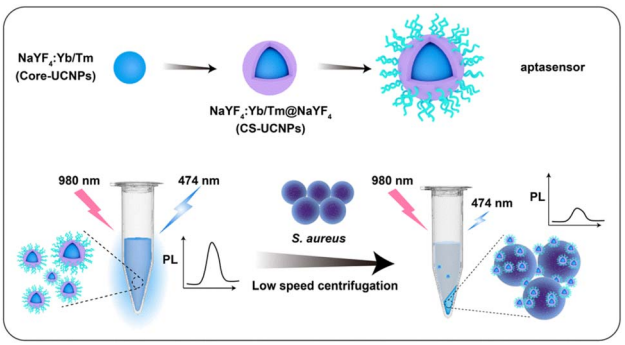

Fig. 1 Schematic illustration of the CS-UCNPs based aptasensor and the detection of *S. aureus*. First, the core UCNPs were synthesized, then the UCNPs were coated with a $NaYF_4$ shell to form CS-UCNPs, and then the aptamer sensor for *S. aureus* detection was prepared by grafting aptamers. The aptamer sensor can bind specifically to *S. aureus* when *S. aureus* is present. After centrifugation at low speed (3000 g, 5 min) and separation precipitation (*Staphylococcus aureus* and bound aptasenors), the fluorescence of the solution was significantly reduced.

Materials and methods

Materials and characterization

Oleic acid (OA), 1-octadecene, yttrium(III) chloride hexahydrate ($YCl_3 \cdot 6H_2O$), ytterbium(III) chloride hexahydrate ($YbCl_3 \cdot 6H_2O$), and thulium(III) chloride hexahydrate ($TmCl_3 \cdot 6H_2O$) were bought from Sigma-Aldrich (St. Louis, USA). Methanol, sodium chloride (NaCl), and sodium hydroxide (NaOH) were purchased from Sinopharm Chemical Reagent Co., Ltd (Shanghai, China). Ammonium fluoride (NH_4F) was acquired from Macklin (Shanghai, China). Agar, Baird-Parker culture medium, potassium tellurite egg yolk reagent and Gram stain kit were bought from Solarbio (Beijing, China). Yeast extract and tryptone were purchased from Thermo Fisher Scientific (MA, USA). All chemicals were of analytical grade or better and used without further purification. Deionized water was used in all experiments. The nucleotide with the following sequence: 5′-SH-C6-GCAATGGTACGGTACTTCCTCGGCACGTTCTCAG-TAGCGCTCGCTGGTCATCCCA-CAGCTACGTCAAAAGTGCACGCTACTTTGCTAA-3′ (*S. aureus* aptamer) and nuclease-free water were purchased from Sangon Biotechnology Inc. (Shanghai, China). *Staphylococcus aureus* (ATCC 29213) and *Escherichia coli* (ER2738) were obtained from

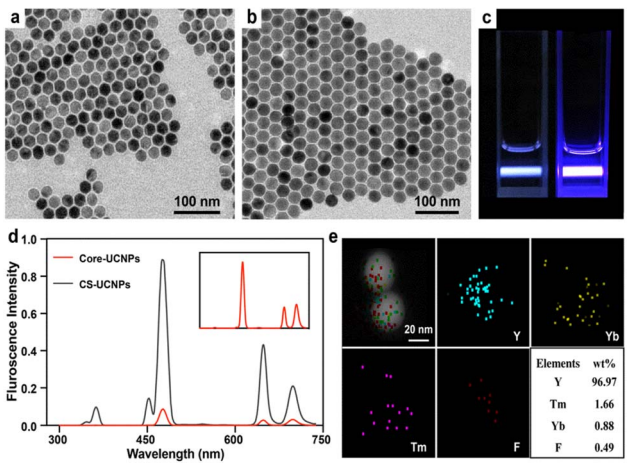

Fig. 2 Characterization of UCNPs and CS-UCNPs. (a and b) TEM images of the core-UCNPs (a) and CS-UCNPs (b). (c) Photographs of core-UCNPs (left) and CS-UCNPs (right) in the cyclohexane solution under the same 980 nm laser excitation. (d) Luminescence properties of core-UCNPs (red line) and CS-UCNPs (black line). (e) High-angle annular dark-field scanning transmission electron microscopy (HAADF-STEM) image and its corresponding elemental contents of CS-UCNPs.

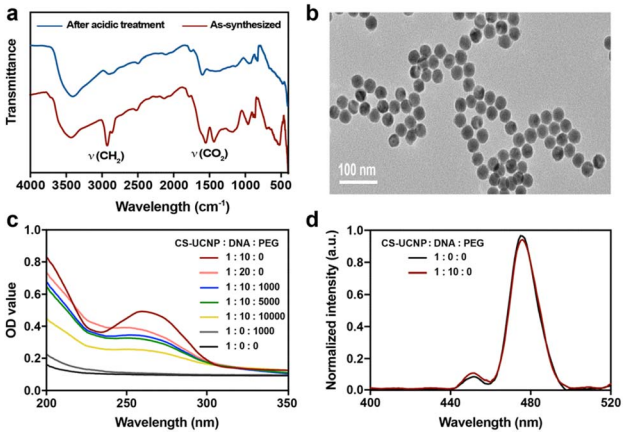

Fig. 3 Modification of CS-UCNPs. (a) FTIR spectra of prepared CS-UCNPs (red line) and OA-removed CS-UCNPs (blue line). (b) TEM image of water-soluble CS-UCNPs. (c) UV-vis absorption spectra of CS-UCNPs and aptamer-modified CS-UCNPs. (d) Normalized fluorescence spectra of CS-UCNPs and aptamer-CS-UCNPs conjugates.

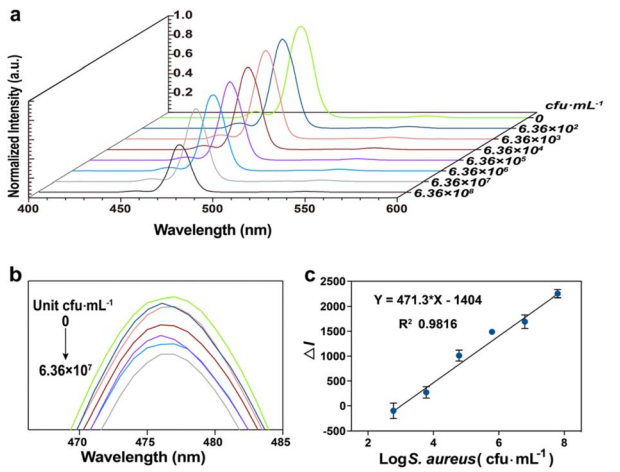

Fig. 4 Sensitivity of CS-UCNPs based aptasensor for *S. aureus* detection. (a and b) Recording output for the detection of different concentrations of *S. aureus* by the CS-UCNPs-based aptasensor. (c) Standard curve of the decreased luminescence intensity ($\Delta I = I_0 - I$) *versus* the concentrations of *S. aureus*.

ATCC (USA). *Salmonella* (isolated strain) and *Enterococcus faecalis* (isolated strain) were isolated and stored by our lab.

Core UCNPs, core–shell UCNPs, water-soluble core–shell UCNPs, aptasensor and the specificity of aptasensor were characterized using TEM. Elemental mapping and data of core–shell UCNPs and aptasensor were obtained *via* Titan Chemi STEM. A full-featured fluorescence spectrometer (FLS920, Edinburgh Instruments) equipped with an external 980 nm laser at a pump power of 3 W confirmed the luminescence spectra. The ligands on the surface of core–shell UCNPs were confirmed by Fourier transform infrared spectroscopy (FTIR) according to our previous method.[17] Absorption spectra were recorded on a SpectraMax M2/M2e spectrometer.

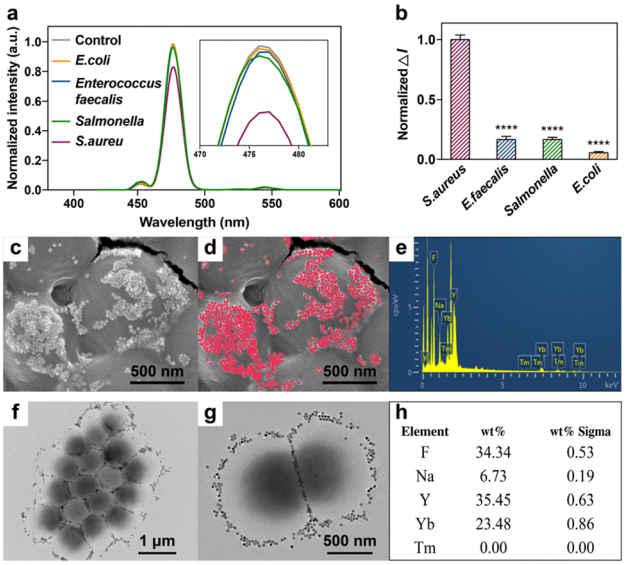

Fig. 5 Specificity of CS-UCNP-based aptasensor for *S. aureus* detection. (a) Normalized fluorescence spectra of the CS-UCNP-based aptasensor in the presence of different bacteria. (b) Normalized decreased upconversion luminescence intensity ($\Delta I = I_0 - I$) of the aptasensor for different bacteria detection (the concentration of all bacteria is 10^3 CFU mL^{-1}). (c and d) SEM images of aptasensor-*S. aureus* conjugates, while the CS-UCNPs are colored in red (d). (f and g) TEM images of aptasensor-*S. aureus* conjugates. (e and h) Elemental contents of aptasensor-*S. aureus* conjugates, which confirmed the nanoparticles were CS-UCNPs.

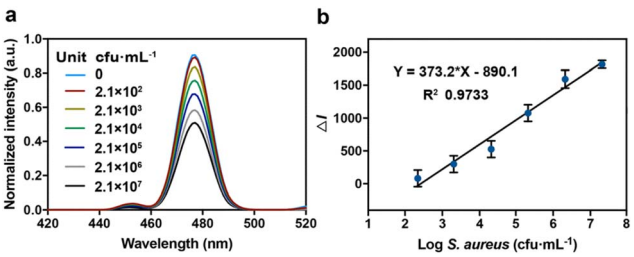

Fig. 6 Detection of *S. aureus* in the milk sample. (a) Normalized fluorescence spectra of the simultaneous detection of different concentrations of *S. aureus* (2.1×10^2–2.1×10^7 CFU mL^{-1}) in milk sample by the CS-UCNP aptasensor. (b) The linear relationship between the decreased fluorescence relative intensity and the logarithm of *S. aureus* concentration with the range of 2.1×10^2–2.1×10^7 CFU mL^{-1}.

Synthesis of core–shell UCNPs

The core UCNPs were synthesized by our previously published methods with different components,[18] YCl_3 (0.747 M), $YbCl_3$ (0.25 M) and $TmCl_3$ (0.003 M). The core–shell UCNPs (CS-UCNPs) were synthesized according to a layer-by-layer method.[19] Briefly, $YCl_3 \cdot 6H_2O$ (0.75 M), $YbCl_3 \cdot 6H_2O$ (0.18 M) and $TmCl_3 \cdot 6H_2O$ (0.003 M) in 1 mL methanol were added into the 1-octadecene (15 mL) and OA (6 mL) solvent. After stirring 750 rpm for 10 min, heated the mixture in the order of 110 °C for 30 min to remove the methanol, 150 °C for 40 min to dissolve the lanthanides, cooling down to 60 °C for 10 min,

Table 1 CS-UCNP based aptasensor and Baird-Parker plate count method for the detection of *S. aureus* of chicken muscle samples

No.	Aptasensor (CFU g^{-1})	BP plate (CFU mL^{-1})
1	27 334	27 300
2	4273	4270
3	1893	1870
4	1632	1620
5	80	73
6	—	12
7	—	7

Table 2 Detection limit and time of different *S. aureus* detection methods

Methods	LOD (CFU mL^{-1})	Time (h)	Reference
Immunochromatographic assay	0.9	25	28
MALDI-MS	7×10^4	1.3	29
Colorimetric sensor	1×10^3	1.5	30
Resonance light scattering	1	1.5	31
Optical biosensor	900	12.75	32
Optical biosensor	60	0.58	Our work

adding 2.5 mL NaOH (1 M) and 10 mL NH_4F (0.4 M) slowly, vacuuming and blowing nitrogen for 3 times, heating 300 °C for 1.5 h then cooling down to room temperature. The coating shell steps are similar to steps above with mere two differences which are adding only $YCl_3 \cdot 6H_2O$ (0.75 M) in OA and 1-octadecene and adding prepared UCNP together with 2.5 mL NaOH (1 M) and 10 mL NH_4F (0.4 M). The heating process must be done slowly. Before constructing the aptasensor, we changed the hydrophobic core–shell UCNPs into hydrophilic ones by the same acidic treatment method.[20]

Construction of aptasensor

Core-shell UCNPs, *S. aureus* aptamer and HS-PEG (MW 2K) were mixed in different molar ratios of 1 : 0 : 10 000, 1 : 10 : 0, 1 : 10 : 1000, 1 : 10 : 5000, 1 : 10 : 10 000, 1 : 20 : 0 and 1 : 20 : 10 000. Here, HS-PEG binds to aptamers by forming disulfide bonds and is subsequently modified to positively charged hydrophilic UCNP to form UCNP-PEG-aptamer biosensor (aptaseneor). After stirring 1 h at 1200 rpm, the mixture was centrifuged at 8000 g for 10 min and washed with nuclease-free water. The aptasensor was collected and stored at 4 °C for further use.

Detection of *S. aureus* by using aptasonsor

In brief, 0.1 mM aptasensor was incubated with a decreasing amount of *S. aureus* (start with 6.3×10^7 CFU mL^{-1}) at 37 °C, 180 rpm, for 30 min. The mixture was centrifuged at 3000 g for 5 min. Discard the precipitate, then the upconversion fluorescence of the supernatant was measured. Different bacteria were added to the aptasensor system to replace *S. aureus* with the same protocols to test the specificity of the aptasensor. To detect *S. aureus* from real samples, purchased sterilized milk (sterilization standard followed GB25190) was polluted with different concentrations of *S. aureus* and then analyzed as in the previous procedures. The negative controls were sterilized milk samples. Multiple chicken samples of 25 g each were weighed and cooked at high temperatures and pressed. The sterilized milk samples and cooked chicken samples were tested according to the national standard method (GB4789.10-2016) to confirm that the cooked chicken samples did not contain *S. aureus*. After full homogenization in a sterile environment, 225 mL PBS buffer was added to each sample. The test was carried out using the detection method specified in the national standard method (GB4789.10-2016), and it was confirmed that the cooked chicken samples did not contain *S. aureus*. Artificially randomly add 1 mL of *S. aureus* solution of different concentrations and store at 4 °C overnight. The artificially contaminated cooked chicken samples were diluted with PBS buffer for 10-fold gradient dilution, and three consecutive groups of suitable gradient dilution samples were selected for detection by BSUNP-aptasensor and Baird-Parker plate counting method.

Results and discussion

Characterization of UCNPs

TEM images show the size and morphology of the as-prepared nanoparticles. The core UCNPs had a mean diameter of 26 nm (Fig. 2a). A thin layer of $NaYF_4$ (3 nm) was successfully coated on the core to form a large core–shell UCNPs (CS-UCNPs), with a mean diameter of 32 nm (Fig. 2b). The CS-UCNPs emitted brighter light than core UCNPs under the same excitation by a 980 nm laser (Fig. 2c and d). The atomic compositions of CS-UCNPs were confirmed by elemental mapping (Fig. 2e), indicating that lanthanide ions (Yb^{3+} and Tm^{3+}) were successfully doped in the CS-UCNPs.

Construction of CS-UCNP based aptasensor

To construct an aptasensor capable of detecting *S. aureus*, the hydrophobic CS-UCNPs were treated with hydrochloric acid to become hydrophilic. As shown in Fig. 3a, the oleate ligands were mostly removed after the acidic treatment. However, the size and the morphology of the hydrophilic CS-UCNPs had not changed significantly compared with those before treatment (Fig. 3b). Then, we labeled the aptamer of *Staphylococcus aureus* on the CS-UCNP surface. The UV-vis absorbance of CS-UCNP at 260 nm confirmed the aptamer conjugation (Fig. 3c), and the best reaction molar ratio of nanoparticles and DNA was 1 : 10. The upconversion luminescence of aptamer functionalized CS-UCNPs slightly decreased (Fig. 3d). Thus, these results demonstrated that the aptasensor for detecting *S. aureus* had been constructed successfully.

Sensitivity test of CS-UCNP based aptasensor for detecting *S. aureus*

To detect *S. aureus*, we incubated different concentrations of *S. aureus* with CS-UCNP based aptasensor, Then, low-speed centrifugation was carried out to remove the *S. aureus*

combined aptasensors. The fluorescence intensity of aptasensors decreased with the increase in the *S. aureus* concentration in the range from 6.36×10^2 to 6.36×10^8 CFU mL^{-1} (Fig. 4a, b). Importantly, the corresponding calibration plot of the decreased fluorescence intensity *vs.* the logarithm of *S. aureus* concentration presented a linear regression equation of $y = 471.3x - 1404$ with a square correlation coefficient of 0.98 (Fig. 4c). The limit of detection (LOD) was calculated to be 60 CFU mL^{-1} by the equation of LOD (KS_0/S, where K is a numerical factor chosen according to the confidence level desired, S_0 is the standard deviation (S. D.) of the black measurements ($n = 10$, $K = 3$)).[21,22]

Specificity analysis of CS-UCNP-based aptasensor

The aptamers we used have been previously reported, which had the specific property of distinguishing *S. aureus* from *Staphylococcus epidermidis*, *Escherichia coli* (*E. coli*), *Streptococcus thermophilus* (*S. thermophilus*), *Enterococuus faecalis* (*E. faecalis*), *Salmonella typhimurium* and *Bacillus subtili*.[23,24] Several bacteria, including *S. aureus*, *E. coli*, *E. faecalis* and *Salmonella* were chosen to verify the selectivity of CS-UCNP based aptasensor. Fig. 5a showed the fluorescence intensity of each group. The control group means no bacteria were added to the aptasensor. As shown in Fig. 5b, other groups did not significantly decrease the fluorescence intensity except the *S. aureus* group. It proves that the aptamers in our research retain their original specificity. TEM and SEM images show that the CS-UCNP-based aptasensors could efficiently bind to the surface of *S. aureus* (Fig. 5c, d, f, and g), which is consistent with the results of fluorescence intensity. We further confirmed the binding nanoparticles were CS-UCNPs by using elemental mapping (Fig. 5e and h), suggesting that CS-UCNP can specifically bind to *S. aureus*.

Detecting *S. aureus* in food samples

To study the performance of CS-UCNP-based aptasensors in detecting *S. aureus* present in foods, we chose milk as a representative sample. After the low speed of centrifugation, a gradually decreasing trend in the fluorescence intensity of the solution due to the presence of *S. aureus* (2.1×10^2 to 2.1×10^7 CFU mL^{-1}) was observed (Fig. 6a). A good linearity between the decreased fluorescence intensity and the logarithm of *S. aureus* concentration ($y = 373.2x - 890.1$) was obtained (Fig. 6b). The detection limit was 146 CFU mL^{-1}. These results indicated that the CS-UCNP-based aptasensor could work well in real samples. Furthermore, we compared the real sample (chicken muscle) detection performances of CS-UCNP-based aptasensor with the Baird-Parker plate count method, which is the golden standard detection method of *S. aureus*. Table 1 showed the results of the two methods. The detection results of these two methods showed a high correlation (ESI Fig. 1†), which indicated that the CS-UCNP-based aptasensor can efficiently detect *S. aureus* in real samples.

Discussion

FRET-based biosensors are complex in design. Here we present a simplified method for experimental *Staphylococcus aureus* detection by centrifugation, Using UCNPs as signal agents and *S. aureus*-specific aptamer as recognition agents. The stability and intensity of the fluorophore are of great significance for a signal reporter, thus, we paid much attention to our core–shell structural UCNPs. By using a coating strategy, we significantly enhanced the fluorescence signal of UCNPs. Obviously, the emission waveform had been slightly changed (Fig. 2d). This phenomenon may be caused by the change of the local crystal field, since CS-UCNPs were built on the same $NaYF_4$ host.[25] To enhance the scope of our UCNP-based aptasensors, we tuned the emission of UCNPs by constructing the core–shell structure, choosing the appropriately doped ions and the concentration. Yb^{3+}/Tm^{3+} has been identified as the proper coupling phonon with high upconversion efficiency.[26] Meanwhile, the lattice vibrations of fluoride materials well matched the maximum phonon energy of Yb^{3+}/Tm^{3+}. Finally, the fluorescence intensity of the CS-UCNPs was 11.4 times higher than that of UCNPs without shell structures. We modified SH group at the 5′ of the *S. aureus* aptamer, so that we could easily load the aptamers onto the surface of CS-UCNPs with oleate ligands removed.[27] In addition, the huge differences in size and mass between the bacteria and nanoparticles ensured the separation of them by centrifugation.

Compared to other *S. aureus* sensors, the LOD and detection time of our aptasensor were greatly decreased (Table 2). Additionally, compared with the Baird-Parker plate count method (golden standard), the CS-UCNP-based aptasensor not only has good detection sensitivity (within the detection limit), but also costs much less time. More importantly, our aptasensor has good specificity, which may be attributed to the specific recognition between *S. aureus* and the aptamer. Even if the aptasensor cannot tell the difference between living and dead bacteria, it can be helpful to assess the harmfulness of *S. aureus* in food.

Conclusions

In summary, we successfully constructed a CS-UCNPs-based aptasensor for *S. aureus* detection. The core–shell structure significantly increased the fluorescence intensity, as well as the sensitivity of the aptasensor. The *S. aureus* bound to CS-UCNPs based aptasensor can then be isolated from the detection system by simple low-speed centrifugation. Our aptasensor was easy to be applied and showed good sensing performance in both nuclease-free water, milk, and chicken muscle samples. Furthermore, the CS-UCNP-based aptasensor can be used in a wide field due to its simplicity and low time consumption features, which provides a feasible strategy for detecting *Staphylococcus aureus* by the biosensor.

Conflicts of interest

There are no conflicts to declare.

Acknowledgements

M. Y. acknowledges the support of Zhejiang Provincial Science and Technology Plan (2021C02072-6, LY22E030004), the National Key R&D Program of China (2020YFC1806903), National Science Foundation (81871499, and 32101095), Provincial Key Laboratory Construction Plans (2020E10025), State of Sericulture Industry Technology System (CARS-18-ZJ0501), Plan of National and Zhejiang Provincial Youth Science and Technology Innovation leader ([2020]366 and 2018R52021).

References

1 G. Y. C. Cheung, J. S. Bae and M. Otto, *Virulence*, 2021, **12**, 547–569.
2 N. Ahmad-Mansour, P. Loubet, C. Pouget, C. Dunyach-Remy, A. Sotto, J. P. Lavigne and V. Molle, *Toxins*, 2021, **13**, 677.
3 X. Zhao, C.-W. Lin, J. Wang and D. H. Oh, *J. Microbiol. Biotechnol.*, 2014, **24**, 297–312.
4 A. Martinon and M. Wilkinson, *J. Food Saf.*, 2011, **31**, 297–312.
5 S. K. Samal, M. Dash, H. A. Declercq, T. Gheysens, J. Dendooven, P. Van der Voort, R. Cornelissen, P. Dubruel and D. L. Kaplan, *Macromol. Biosci.*, 2014, **14**, 991–1003.
6 X. Y. Wang, J. Y. Yang, Y. T. Wang, H. C. Zhang, M. L. Chen, T. Yang and J. H. Wang, *Talanta*, 2021, **221**, 121668.
7 W. Gan, Z. Xu, Y. Li, W. Bi, L. Chu, Q. Qi, Y. Yang, P. Zhang, N. Gan, S. Dai and T. Xu, *Biosens. Bioelectron.*, 2022, **199**, 113860.
8 S. Yao, C. Zhao, M. Shang, J. Li and J. Wang, *Food Chem. Toxicol.*, 2021, **150**, 112071.
9 R. Renuka, N. Maroli, J. Achuth, K. Ponmalai and K. Kadirvelu, *Spectrochim. Acta, Part A*, 2020, **243**, 118662.
10 Q. Chen, R. Sheng, P. Wang, Q. Ouyang, A. Wang, S. Ali, M. Zareef and M. M. Hassan, *Spectrochim. Acta, Part A*, 2020, **241**, 118654.
11 Q. Ouyang, L. Wang, W. Ahmad, Y. Yang and Q. Chen, *J. Agric. Food Chem.*, 2021, **69**, 9947–9956.
12 Y. Ma, M. Song, L. Li, X. Lao, M. C. Wong and J. Hao, *Exploration*, 2022, **2**, 20210216.
13 A. V. Lakhin, V. Z. Tarantul and L. V. Gening, *Acta Nat.*, 2013, **5**, 34–43.
14 M. R. Dunn, R. M. Jimenez and J. C. Chaput, *Nat. Rev. Chem.*, 2017, **1**, 1–16.
15 X. Zhu, J. Zhang, J. Liu and Y. Zhang, *Adv. Sci.*, 2019, **6**, 1901358.
16 C. Homann, L. Krukewitt, F. Frenzel, B. Grauel, C. Wuerth, U. Resch-Genger and M. Haase, *Angew. Chem., Int. Ed.*, 2018, **57**, 8765–8769.
17 G. He, Y. Shuai, Y. Hai, T. Yang, X. Pan, Y. Liu, X. Meng, H. Yang, M. Yang and C. Mao, *Mater. Today Nano*, 2022, **20**, 100268.
18 Z. Li, S. Lv, Y. Wang, S. Chen and Z. Liu, *J. Am. Chem. Soc.*, 2015, **137**, 3421–3427.
19 N. J. J. Johnson and F. C. J. M. van Veggel, *Nano Res.*, 2013, **6**, 547–561.
20 W. Kong, T. Sun, B. Chen, X. Chen, F. Ai, X. Zhu, M. Li, W. Zhang, G. Zhu and F. Wang, *Inorg. Chem.*, 2017, **56**, 872–877.
21 W. C. Hazeleger, W. F. Jacobs-Reitsma and H. M. W. Den Besten, *Front. Microbiol.*, 2022, **13**, 834568.
22 D. A. Armbruster and T. Pry, *Clin. Biochem. Rev.*, 2008, **29**(1), S49–S52.
23 X. Cao, S. Li, L. Chen, H. Ding, H. Xu, Y. Huang, J. Li, N. Liu, W. Cao and Y. Zhu, *Nucleic Acids Res.*, 2009, **37**, 4621–4628.
24 Q. Ouyang, Y. Yang, S. Ali, L. Wang, H. Li and Q. Chen, *Spectrochim. Acta, Part A*, 2021, **255**, 119734.
25 S. Ye, G. Chen, W. Shao, J. Qu and P. N. Prasad, *Nanoscale*, 2015, **7**, 3976–3984.
26 G. Chen, C. Yang and P. N. Prasad, *Acc. Chem. Res.*, 2013, **46**, 1474–1486.
27 Y. Zhang, B. Duan, Q. Bao, T. Yang, T. Wei, J. Wang, C. Mao, C. Zhang and M. Yang, *J. Mater. Chem. B*, 2020, **8**, 8607–8613.
28 S.-H. Huang, *Sens. Actuators, B*, 2007, **127**, 335–340.
29 Y. S. Lin, P. J. Tsai, M. F. Weng and Y. C. Chen, *Anal. Chem.*, 2005, **77**, 1753–1760.
30 Y. Zhang, S. Shi, J. Xing, W. Tan, C. Zhang, L. Zhang, H. Yuan, M. Zhang and J. Qiao, *RSC Adv.*, 2019, **9**, 33589–33595.
31 Y.-C. Chang, C.-Y. Yang, R.-L. Sun, Y.-F. Cheng, W.-C. Kao and P.-C. Yang, *Sci. Rep.*, 2013, **3**, 1863.
32 X. Wang, Y. Du, Y. Li, D. Li and R. Sun, *J. Biomater. Sci., Polym. Ed.*, 2011, **22**, 1881–1893.